

Alma Mater Studiorum Università di Bologna
Archivio istituzionale della ricerca

Influence of inorganic anions from atmospheric depositions on weathering steel corrosion and metal release

This is the final peer-reviewed author's accepted manuscript (postprint) of the following publication:

Published Version:

Influence of inorganic anions from atmospheric depositions on weathering steel corrosion and metal release / Bernardi E.; Vassura I.; Raffo S.; Nobili L.; Passarini F.; de la Fuente D.; Morcillo M.. - In: CONSTRUCTION AND BUILDING MATERIALS. - ISSN 0950-0618. - STAMPA. - 236:(2020), pp. 117515.1-117515.12. [10.1016/j.conbuildmat.2019.117515]

Availability:

This version is available at: <https://hdl.handle.net/11585/714220> since: 2020-04-21

Published:

DOI: <http://doi.org/10.1016/j.conbuildmat.2019.117515>

Terms of use:

Some rights reserved. The terms and conditions for the reuse of this version of the manuscript are specified in the publishing policy. For all terms of use and more information see the publisher's website.

This item was downloaded from IRIS Università di Bologna (<https://cris.unibo.it/>).
When citing, please refer to the published version.

(Article begins on next page)

This is the final peer-reviewed accepted manuscript of:

Elena Bernardi, Ivano Vassura, Simona Raffo, Lara Nobili, Fabrizio Passarini, Daniel de la Fuente, Manuel Morcillo, *Influence of inorganic anions from atmospheric depositions on weathering steel corrosion and metal release*, Construction and Building Materials 236 (2020) 117515

The final published version is available online at:

<https://doi.org/10.1016/j.conbuildmat.2019.117515>

Rights / License: CC-BY-NC-ND 4.0 license

(<http://creativecommons.org/licenses/by-nc-nd/4.0/>)

The terms and conditions for the reuse of this version of the manuscript are specified in the publishing policy. For all terms of use and more information see the publisher's website.

This item was downloaded from IRIS Università di Bologna (<https://cris.unibo.it/>)

When citing, please refer to the published version.

This is the pre-copyedited, author-produced version of the final peer-reviewed accepted manuscript of “E. Bernardi et al., Influence of inorganic anions from atmospheric depositions on weathering steel corrosion and metal release, Construction and Building Materials 236 (2020) 117515”. The final published version is available online at: <https://doi.org/10.1016/j.conbuildmat.2019.117515>. When citing, please refer to the published version.

Influence of inorganic anions from atmospheric depositions on weathering steel corrosion and metal release

Elena Bernardi^{a,b,*}, Ivano Vassura^{a,b}, Simona Raffo^a, Lara Nobili^a, Fabrizio Passarini^{a,b}, Daniel de la Fuente^c, Manuel Morcillo^c

^a Department of Industrial Chemistry “Toso Montanari”, University of Bologna, Viale del Risorgimento 4, 40136 Bologna, Italy; *elena.bernardi@unibo.it

^b Interdepartmental Center for Industrial Research (CIRI) Energy and Environment, University of Bologna, Via Angherà 22, 47900 Rimini, Italy

^c National Centre for Metallurgical Research (CENIM-CSIC), Avda. Gregorio del Amo, 8, 28040 Madrid, Spain

Abstract:

The individual effects of nitrate, chloride and sulphate on weathering steel appearance, patina composition, corrosion rate and metal release (Fe, Cr, Mn, Cu, Ni) were investigated by accelerated ageing with anion solutions at environmental concentrations. The anions influence the growth and evolution of corrosion products in the following order: $\text{SO}_4^{2-} > \text{Cl}^- > \text{NO}_3^-$. Even though SO_4^{2-} induces the highest kinetic in patina growth and metal release, it tends to passivate the alloy by suppressing both processes with increasing time and concentration. Cl^- , conversely, does not induce any stabilization trend and seems to contribute more than the other anions to metal runoff.

Keywords: atmospheric corrosion; Cor-Ten A; metal dissolution; rust; alternate immersions; Cebelcor Test; Principal Component Analysis (PCA)

1. Introduction

Metals and alloys exposed to the atmosphere suffer a natural and spontaneous degradation, known as atmospheric corrosion, which causes aesthetic and structural damages with high associated costs [1]. To solve these problems, beside protective strategies, new classes of materials were developed during the XX century. One of these is composed of high-strength low-alloy steels with improved atmospheric corrosion resistance, known as weathering steels. Weathering steels (WS) are characterized by low carbon content (<0.2 wt%) and small amounts (< 5 wt% in total) of specific alloying elements such as Cr, Cu, Mn, Ni, P [2]. They show a higher corrosion resistance compared to plain carbon steel and, in atmospheres of low corrosivity (C2–C3), do not require to be painted due to the formation of an adherent auto-protective and aesthetically pleasant rust layer, often called “patina” [3]. For this reasons WS are widely used worldwide for the construction of highway structures, bridges, power poles, cladding of building facades, urban furnishing or artistic sculptures.

The patina evolves and increases its protective ability over time, stabilizing in the order of years/decades, according to the exposure environment. The protective rust mainly consists of an oxide double layer: the outermost contains lepidocrocite ($\gamma\text{-FeOOH}$) and goethite ($\alpha\text{-FeOOH}$); the innermost closely packed nano-phase goethite and Cr-substituted goethite. Goethite has a pseudo tunnel structure and, in the inner layer, the higher concentration of Cr and Ni influences the evolution of the network, leading to a dense aggregation of fine crystals able to hinder the entrance of aggressive anions due to their cation selectivity. In order to form an effective protective rust, weathering steel also requires specific exposure conditions related to both the environment and the design, i.e. cyclic periods of wetting by rain followed by fast drying, no water or moisture stagnation and weakly aggressive atmospheres. [3,4]

As regards the atmosphere of exposure, chloride (Cl^-) and sulphur dioxide (SO_2) are recognized as the main aggressive species for weathering steel [3]. Cl^- easily penetrates through the rust and promotes the formation

and stabilization of akageneite (β -FeOOH). This oxyhydroxide has a tunnel structure that works as reservoir of Cl^- and contributes to develop a non-protective rust [5]. SO_2 , if lower than $20 \text{ mg}_{\text{SO}_2} \text{ m}^{-2} \text{ d}^{-1}$, accelerates the stabilization of the corrosion rates within acceptable levels. Higher SO_2 amounts significantly increase WS corrosion [4]. During the last decades, the significant reduction in SO_2 levels in most of the world has led to investigate also the influence of O_3 , NO_x and particulate matter on WS corrosion [6–9]. However, while the action of single and mixed atmospheric gases has been well studied, relatively few works [8,9] specifically investigated the effects of particulate matter and salts deposition on this alloy. Moreover, if the role of Cl^- was extensively considered in regard to the corrosion rate and patina composition, the relative contribution of Cl^- , NO_3^- and SO_4^{2-} has been evaluated only for mild steel corrosion [10] or in relation to the synthesis of artificial steel rust starting from Fe(II) or Fe(III) solutions [11–14]. The effects that the ions contained in atmospheric depositions have on corrosion are currently an important research topic. In fact, changes in pollutant emissions and climate change affect each other, possibly leading to changes in concentrations and relative proportions between the ions [15].

This work aims to investigate and compare the individual contribution of the main anions contained in the atmospheric depositions, i.e. NO_3^- , Cl^- and SO_4^{2-} , to weathering steel corrosion and metal release. To this aim, specimens of weathering steel were aged by the Cebelcor test, an immersion-emersion cyclic test frequently used for atmospheric corrosion studies [16,17]. It was run for a total of 20 days (522 cycles) using solutions of each single anion at different concentrations as weathering media. Concentrations were chosen to simulate exposure to mild and quite aggressive atmospheric depositions. The effects of each anion were evaluated through (i) the characterization of the rust layer formed, (ii) the quantification of corrosion rate and (iii) the quantification of the alloying metals retained in rust or released in solution, either in dissolved or particulate form.

2. Materials and Methods

2.1 Material

A commercial weathering steel, analogous to Cor-Ten A, was tested. Specimens ($5 \times 5 \times 0.2 \text{ cm}$) were supplied by Kalikos International srl.

The measured steel composition is reported in Table 1. Carbon and sulphur were quantified by a C/S Analyzer equipped with induction furnace and IR absorption cells, while other elements were quantified by Glow Discharge Optical Emission Spectroscopy (GD-OES).

Table 1. Elemental composition (weight %) of the weathering steel tested.

C	Si	Mn	P	S	Cr	Ni	Cu	Fe
0.085	0.44	0.38	0.091	0.022	0.80	0.17	0.30	~ 97.7

The microstructure of the alloy was observed by a Nikon EPIP-HOT 300 polarized light microscope after incorporation in epoxy resin, polishing and chemical etching by a 2% Nital solution (HNO_3 2% – EtOH 98%). The microstructure appears uniform (Figure S1 in Supplementary Information): ferrite and pearlite can be observed in both the longitudinal and transversal directions. Pearlite is present in very fine grain size and in globular form, the latter suggesting that heat treatments occurred during alloy processing [18].

Before the test, each specimen was measured by calliper, degreased with a toluene-based solvent (Kelsia), washed with water, dried and weighted (0.1 mg of sensitivity).

2.2 Weathering Solutions

According to the aim of the study, nine different solutions containing nitrate, chloride or sulphate at three concentration levels (1.5 , 10 and 25 mg L^{-1}) were used for the accelerated ageing (Table 2).

The concentration levels were selected within a range defined on the basis of the average ion concentrations and fluxes recorded for atmospheric depositions in different sites in the world. The sites taken into account were chosen in order to be representative of mild to quite aggressive environments; among the most significant those reported in [19–23] can be mentioned.

NO_3^- , Cl^- and SO_4^{2-} solutions were prepared by weighing the appropriate amount of the corresponding sodium salts in order to minimize any effect related to different counterions. For all the weathering solutions, initial pH values ranged between 5.4 – 5.5.

Table 2. Weathering solutions used for the Cebelcor ageing test.

Anion		NO_3^-			Cl^-			SO_4^{2-}		
Anion concentration	(mg L ⁻¹)	1.5	10	25	1.5	10	25	1.5	10	25

2.3 Cebelcor test and experimental plan

The Cebelcor test is a wet and dry accelerated corrosion test developed by M. Pourbaix [16]. By alternating periods of immersion in a weathering solution, emersion and drying, it can simulate cyclic exposure to stagnant rainwater or high humidity.

The test was performed through an automatic equipment [24] designed by the CAPA (Corrosión Atmosférica/Pinturas Anticorrosivas) group of the National Centre for Metallurgical Research - CENIM (Madrid, Spain) according to the methodological requirements described by M. Pourbaix (Figure S2). Weathering solutions, placed in glass containers holding up to four specimens at the same time, are maintained well aerated by water pumps (flow rate of 300 L/h). Drying is ensured by exposing the specimens to infrared radiation (100 W IR lamps) at a temperature of 50 °C.

54-minute cycles were set, alternating 12 minutes of immersion with 42 minutes of emersion and drying, so that the wetting time of the steel surface corresponds to 22% of the ageing time. The Cebelcor test was run for a total of 522 cycles (20 days). The experimental plan is given in Figure 1 and described in the following. Four WS specimens were contemporary aged in each weathering solution (about 3 L). When necessary, water lost by evaporation was replenished to maintain the volume constant. After 143, 276, 408 and 522 cycles (corresponding to 5, 10, 15 and 20 days of ageing, respectively), representative aliquots of each solution, before and after filtration on cellulose acetate membrane (0.45 µm pore-size), were sampled and analysed in order to determine metals released in the total (TRF), dissolved (DF) and particulate (PF) fractions (section 2.5). After each sampling, weathering solutions were renewed.

After 276 and 522 cycles, two specimens for each solution were removed. One of them was employed for surface characterization (section 2.4). The other one (together with a non-aged specimen as reference) underwent pickling in a solution of HCl (50%) and hexamethylenetetramine, according to ISO 8407 [25], for mass loss (ML) determination and corrosion rate (v_{corr}) calculation. The pickling solutions, containing the dissolved adherent rust (AR) were sampled and analysed (section 2.5) to determine the metal content in patinas.

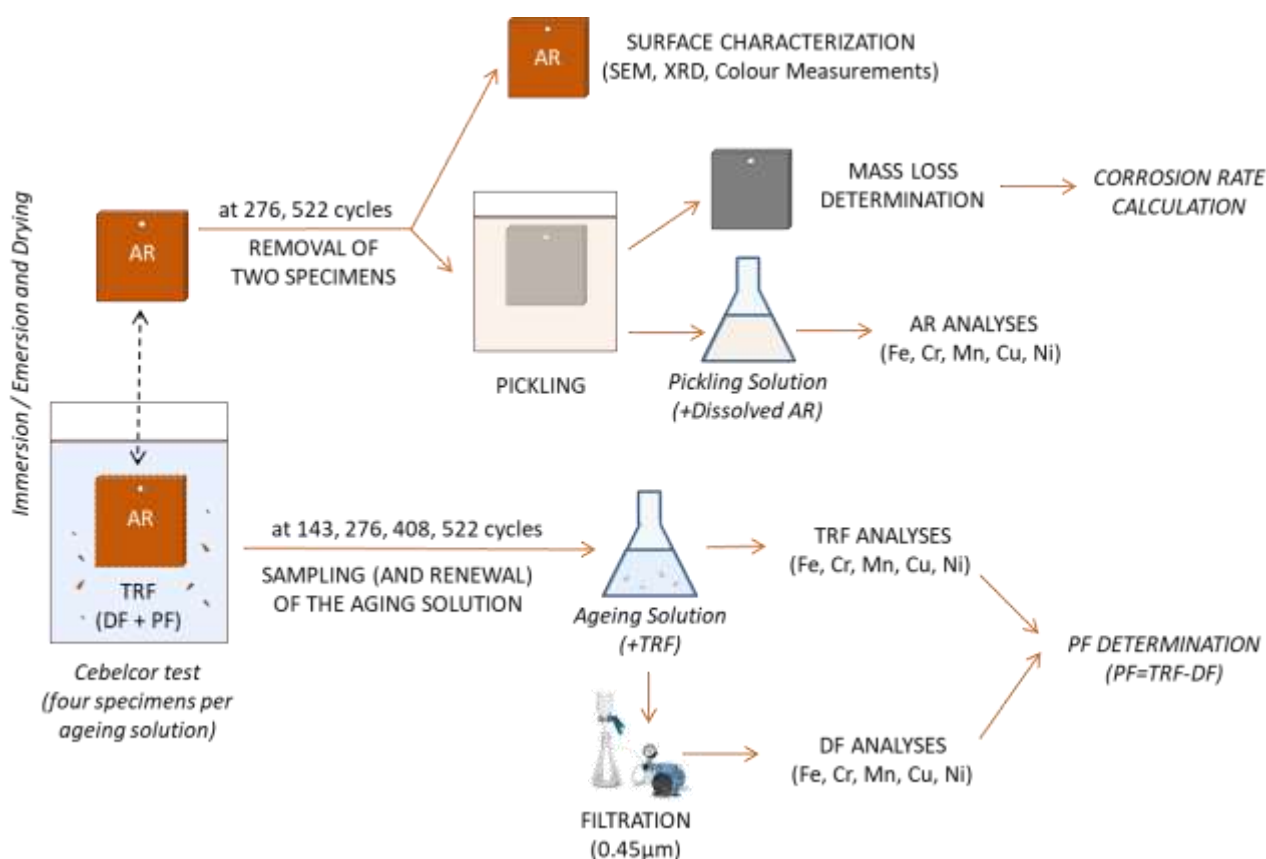


Figure 1. Scheme of the experimental plan. The same operational sequence was repeated for each weathering solution. Metals (Fe, Cr, Mn, Cu, Ni) were analysed in the following fractions: Adherent Rust (AR); Total Released Fraction (TRF); Dissolved Fraction (DF). Metals in Particulate Fraction (PF) were calculated as difference: $PF = TRF - DF$.

2.4 Surface characterization

The morphology and composition of the WS patinas were examined by means of Scanning Electron Microscopy (SEM) and X-ray diffraction (XRD) analysis.

SEM analyses were performed through a high-resolution JEOL JXA-840 electron microscope equipped with a link system electron microprobe by applying the following conditions: working distance = 10 mm; accelerating voltage between 5 and 7 keV.

XRD patterns were recorded through a Bruker AXS diffractometer – D8 Advance, equipped with cobalt X-ray tube ($\lambda = 1.79 \text{ \AA}$) and diffracted beam monochromator; data were collected in steps of 0.03° over the $10\text{--}80^\circ$ 2θ range, with a time per step of 3 seconds. Quantification of the crystalline phases present in the rust was carried out from the XRD patterns using the Rietveld method. To this aim, version 4.2 of the TOPAS Rietveld analysis software (Bruker AXS) was used to model the full pattern with the crystallographic information obtained from Pearson's Crystal Structure database.

In addition, aesthetical evaluation and colorimetric measurements were performed, before and after the ageing test, through a Datacolor D400 spectrophotometer (D65 illuminant, 10° observer, beam of diffuse light of 9 mm, specular component excluded). At least three measurements were performed on each specimen and data were elaborated in the CIELAB colour space, where the difference between two colours is expressed by the ΔE parameter: $\Delta E = \sqrt{(\Delta L^*)^2 + (\Delta a^*)^2 + (\Delta b^*)^2}$, being L^* , a^* and b^* the lightness, the red/green and the yellow/blue axis, respectively.

2.5 Metal analysis

Fe, Cr, Mn, Cu and Ni released in the weathering solutions or retained in the rust were periodically determined. According to the experimental plan (Figure 1), the following fractions were quantified:

a) Metal released in solution as Total Released Fraction (TRF). This fraction includes metal in both dissolved and particulate form. It was determined by analysing a representative aliquot of the weathering solutions acidified with HNO_3 65% suprapur until complete dissolution of the particulate fraction.

b) Metal released in solution as Dissolved Fraction (DF). This fraction was determined by filtering (0.45 μm pore-size), acidifying with HNO_3 65 % suprapur until $\text{pH} < 2$, and analysing a representative aliquot of the weathering solutions.

c) Metal released in solution as Particulate Fraction (PF). This fraction can include both Non-Adherent Rust (NAR), not soluble corrosion products poorly adherent to the surface and lost in the ageing environment, and metal eventually precipitating as not soluble species at the pH -level of weathering solution. PF was calculated by subtracting DF to TRF.

d) Metal contained in the final Adherent Rust (AR), here considered as all the corrosion products that remained bound to the metal surface during the ageing. This fraction was determined by analysing the pickling solutions of aged and non-aged specimens.

Fe, Cr, Mn, Cu and Ni in the weathering and pickling solutions were analysed by Perkin Elmer PinAAcle900z Atomic Absorption Spectrometer with electro-thermal atomizer. Limit of Detection (LoD) were determined as the metal concentration corresponding to 3 times the standard deviation of 20 replicates of a blank solution (LoD, $\mu\text{g L}^{-1}$: Fe 0.8; Cr 0.2; Mn 0.2; Cu 0.3; Ni 0.6). Three replicate readings were performed on each sample and quality control standard analyses were performed every ten samples.

2.6 Multivariate data analysis

Experimental results were analysed by Principal Component Analysis (PCA), in order to globally consider the effects of the ageing conditions on weathering steel corrosion. In fact, compared to the univariate approach, this explorative method allows to analyse together all the variables acting on a process and to isolate only the relevant information, minimizing redundant data.

The experimental dataset consists in 9 objects (corresponding to the 9 tested solutions) and 11 variables connected to them (mass loss, Fe, Cr, Mn, Cu, and Ni cumulatively released in solution and retained in patinas at the end of ageing). Data were processed using The Unscrambler v. 10.3 (CAMO AS, Norway). Before the PCA was run, data were pre-treated through centering and scaling processes. According to the Scree Test, four principal components were chosen, giving an explained variance of 97%.

3. Results and Discussion

3.1 Characterization of corrosion products

Appearance, morphology and composition of corrosion layers formed after Cebelcor test provide first information about the effects of the different anions on weathering steel corrosion (content of single metals in the corrosion layers will be discussed in section 3.3).

Patinas visually differ in both uniformity and colour, depending on test time and, mainly, on composition and concentration of the ageing solutions (Figure S3). In fact, as expected, patinas increase surface coverage over time, but with significant differences between solutions. Specimens aged in NO_3^- at the lowest and intermediate concentration (1.5 and 10 mg L^{-1}) always show large poorly corroded areas where the underlying alloy is still visible through the patina. Only after 522 ageing cycles at the highest concentration (25 $\text{mg L}^{-1} \text{NO}_3^-$) the surfaces result completely covered. In Cl^- , the underlying alloy remains always partly visible at the lowest concentration (1.5 $\text{mg L}^{-1} \text{Cl}^-$), while a complete visual coverage is reached after 276 cycles at the intermediate and highest concentration (10 and 25 $\text{mg L}^{-1} \text{Cl}^-$). In SO_4^{2-} a complete coverage is reached after 276 cycles even at a concentration of 1.5 $\text{mg L}^{-1} \text{SO}_4^{2-}$.

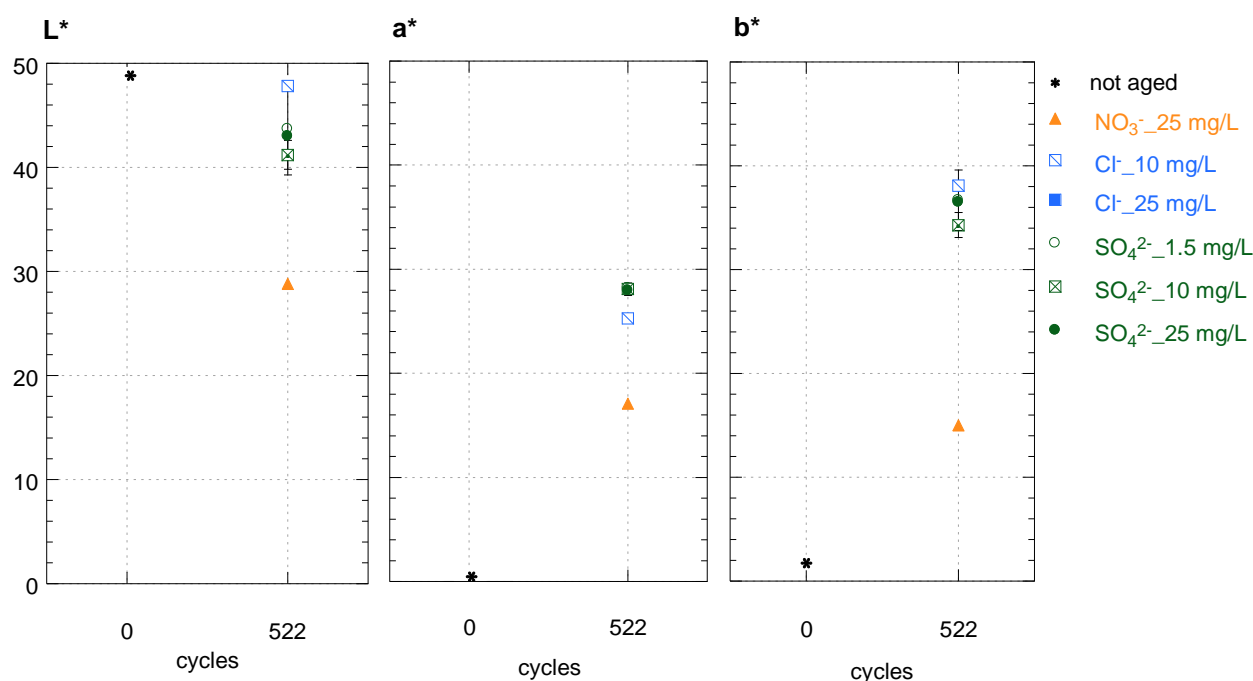


Figure 2. L^* , a^* and b^* values recorded on WS specimens before and after the ageing (522 Cebelcor cycles) in NO_3^- , Cl^- and SO_4^{2-} solutions at different concentrations. Only specimens completely covered by the patina were analysed.

Colour measurements were performed at the end of the ageing only on specimens with a complete visual coverage (Figure 2). The colour change (ΔE) of specimens in Cl^- and SO_4^{2-} solutions is close to 45 colour units and mainly influenced by changes in a^* and b^* parameters: patinas appear brown/orange, with those developed in SO_4^{2-} slightly darker and more red. Specimens aged in NO_3^- undergo a lower colour change (ΔE about 30) but, in this case, it is due to significant variations also in lightness. Patinas result therefore darker and less orange than those developed in Cl^- and SO_4^{2-} .

From a morphological point of view, at the end of the ageing in NO_3^- at the highest concentration (25 mg L^{-1}), two different characteristic areas can be distinguished by SEM analyses (Figure 3). The first area (Figure 3a1) is characterized by lamina formations with a feather-like appearance, while the second one (Figure 3a2) by the presence of flowery and hexagonal crystals. In a previous study, the correspondence morphology-phase for the most common rust morphologies was obtained by means of the combined SEM/Micro-Raman technique [26]. According to this study, all these different morphologies are typical of lepidocrocite, the iron oxide-hydroxide generally growing in the first stages of WS corrosion. In the second area also rounded sheets typical of hematite [26] are present. At the same time of ageing and concentration, Cl^- and SO_4^{2-} solutions lead to more evolved corrosion layers (Figure 3b,c): surfaces are completely covered by sandy and flowery crystals, probably of lepidocrocite [26]. Crystals that grow in the SO_4^{2-} solution (Figure 3c) show a larger average diameter ($\sim 20 \mu\text{m}$) and lead to a more porous patina than those growing in the Cl^- solution (Figure 3b), where the formation of agglomerates of smaller crystals ($\sim 10 \mu\text{m}$) is promoted.

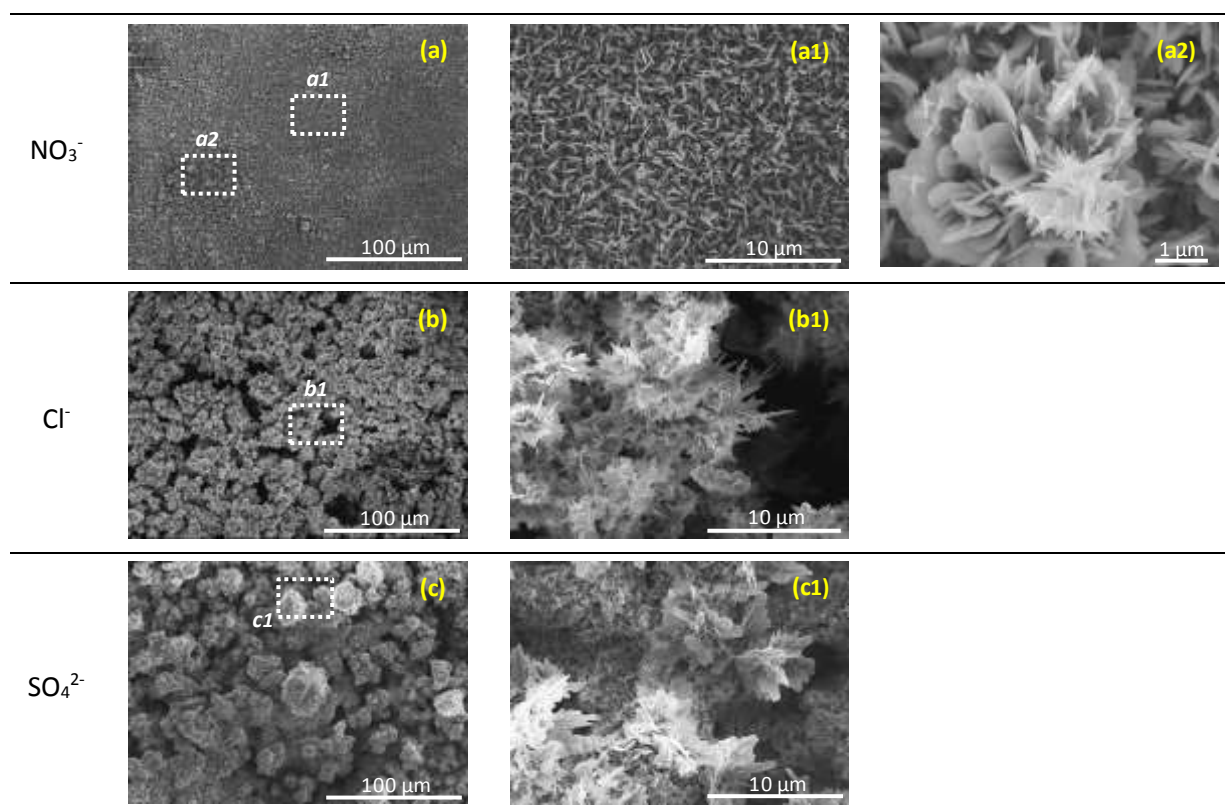


Figure 3. SEM images of WS specimens aged in 25 mg L⁻¹ NO₃⁻ (a), Cl⁻ (b) and SO₄²⁻ (c) solutions for 522 Cebelcor cycles.

The presence of the products hypothesized on the basis of SEM observation was confirmed by XRD analyses. Lepidocrocite was the main product detected by XRD at the end of the ageing in all the weathering solutions at the highest concentration (Table 3, Figure S4). Hematite was also detected in relative percentages ranging from ~12% in SO₄²⁻ to ~23% in NO₃⁻. In NO₃⁻ and Cl⁻, lepidocrocite and hematite were the only revealed products, with hematite increasing with Cl⁻ concentration (Table 4) and time (e.g. from 11% to 19% after 276 and 522 cycles in Cl⁻ 25 mg L⁻¹, respectively).

Table 3. Corrosion products and relative proportions (%) identified by XRD analysis on WS specimens aged in 25 mg L⁻¹ NO₃⁻, Cl⁻ and SO₄²⁻ solutions for 522 Cebelcor cycles.

	Lepidocrocite	Hematite	Magnetite	Goethite
NO ₃ ⁻ 25 mg L ⁻¹	77.4	22.6	-	-
Cl ⁻ 25 mg L ⁻¹	80.7	19.3	-	-
SO ₄ ²⁻ 25 mg L ⁻¹	64.6	12.8	15.0	7.6

Table 4. Corrosion products and relative proportions (%) identified by XRD analysis on WS specimens aged in 1.5 mg L⁻¹, 10 mg L⁻¹ and 25 mg L⁻¹ Cl⁻ solutions for 522 Cebelcor cycles.

	Lepidocrocite	Hematite
Cl ⁻ 1.5 mg L ⁻¹	86.1	13.9
Cl ⁻ 10 mg L ⁻¹	85.6	14.4

Cl⁻ 25 mg L⁻¹	80.7	19.3
--	-------------	-------------

The presence of hematite, usually not commonly detected in field exposure, can be explained by the experimental conditions here applied. In particular, according to Cornell and Schwertmann [27], pH of the weathering solutions varying cyclically from 5.4 to 7 during the ageing, and temperature reached during the drying phase (50 °C) can have favoured its formation.

It is interesting to notice that specimens aged in Cl⁻ solutions do not exhibit traces of akaganeite (β-FeOOH), due to the low Cl⁻ concentrations which WS specimens were exposed to. In fact, a minimum Cl⁻ concentration of 2-4 mol L⁻¹ is necessary for the formation of akaganeite [28,29] and, in atmosphere, an annual average deposition rate of about 60 mg_{Cl}·m⁻²·day⁻¹ seems to be required [30]. It has to be considered that Cl⁻ could accumulate on the specimens during the wet-dry cycles, but the slight washing effect due to the mechanism of extraction of the specimens from the weathering solution could also have hindered the growth of akaganeite. In fact, it was demonstrated that, at low Cl⁻ deposition rate (i.e. 118.2 mg m⁻² of Cl⁻ per ageing cycle, obtained by spraying 0.005M NaCl on the specimens), repeated wet-dry cycles with some washing effect result disadvantage for akaganeite formation [31].

Goethite, one of the products responsible for patina compactness and cohesion, was detected only on specimens aged for 522 cycles in SO₄²⁻ 25 mg L⁻¹ (Table 3, Figure S4). This confirms the ability of sulphates to promote goethite formation [12,27], that in natural environment seems to proceed through transformation from lepidocrocite [4]. These specimens also present a significant amount (~15%) of magnetite, usually found in WS exposed outdoor [5].

Results from surface characterization suggest that, at the considered concentrations, the anions promote the growth and evolution of corrosion products in the following order: SO₄²⁻>Cl⁻>NO₃⁻.

3.2 Corrosion rates

The corrosion rate (v_{corr}) of the specimens was calculated in mg cm⁻² d⁻¹ by dividing the mass loss (section 2.3) by the surface area and the days of ageing. Corrosion rates (Figure 4) show different trend with concentration and time depending on the weathering anion.

In NO₃⁻ solutions v_{corr} are always one order of magnitude lower than in the corresponding Cl⁻ and SO₄²⁻ solutions, confirming the general lower aggressiveness of this anion suggested by surface analyses. v_{corr} remains stable around 0.025 mg cm⁻² d⁻¹ and only when a concentration and time threshold (corresponding to around 25 mg L⁻¹ and 522 cycles) is reached, NO₃⁻ seems to start to influence the corrosion process, reaching a v_{corr} of 0.08 mg cm⁻² d⁻¹.

In Cl⁻ solutions, at the same ageing time, v_{corr} linearly increases with Cl⁻ concentration ($r^2 > 0.998$) and, at the same concentration, it remains quite constant over time, suggesting that Cl⁻ does not induce any stabilization of the corrosion trend.

In SO₄²⁻ solutions the highest corrosion rates are generally recorded, but v_{corr} show a clear tendency to slow down with increasing concentration and time. In fact, at the same ageing time, the increase in concentration induces a logarithmic v_{corr} increase ($r^2 > 0.984$). At the same concentration, the doubling in ageing time induces a v_{corr} decrease of about 35% on average. This could be partly related to the formation of goethite that, even if in small percentages (~8%), was only revealed in patinas developed in SO₄²⁻.

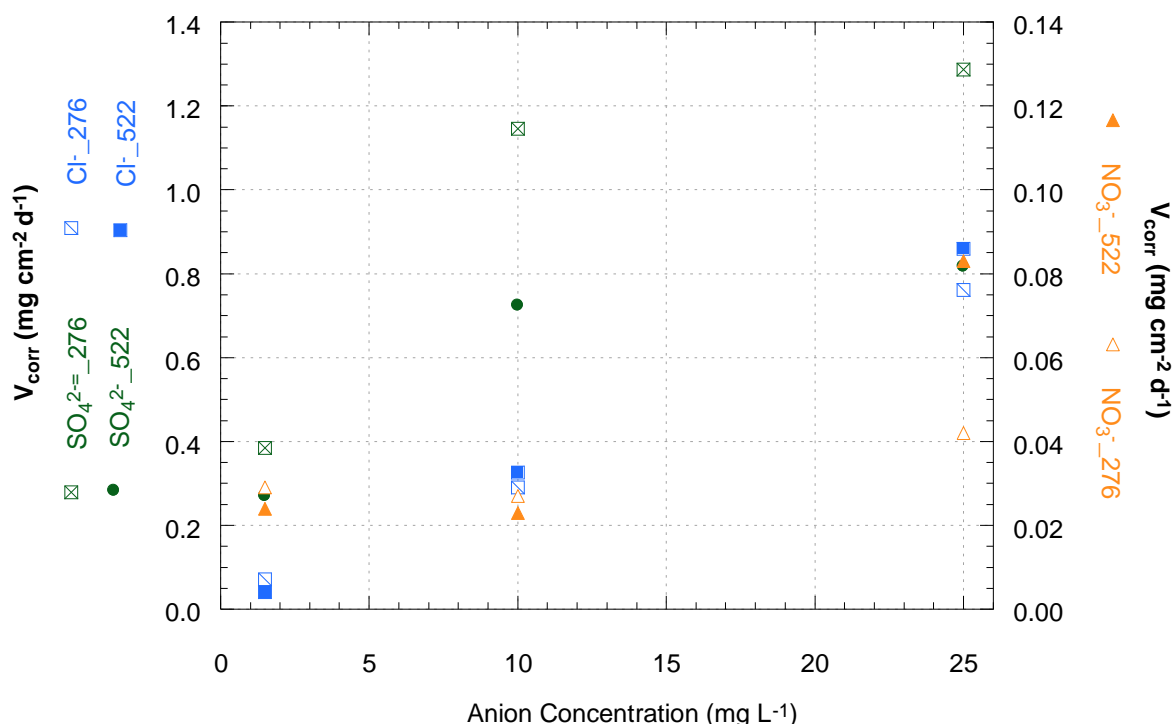


Figure 4. Corrosion rate (v_{corr} ; $\text{mg cm}^{-2} \text{d}^{-1}$) of WS specimens aged in NO_3^- , Cl^- and SO_4^{2-} solutions for 276 and 522 Cebelcor cycles, corresponding to 10 and 20 days of ageing.

3.3 Oxidized metals: retention in patina and release in solution

The influence of the anions on the tendency of oxidized metals (Fe, Cr, Mn, Cu, Ni) to remain in the adherent rust or to be released in solution was evaluated. Metals were determined in different fractions (Adherent Rust-AR, Total Released Fraction - TRF, Dissolved Fraction - DF, Particulate Fraction - PF), according to definitions and procedures reported in section 2.5.

A preliminary mass balance check was performed by comparing the sum of metals in AR and TRF to mass loss: a 30% difference was assumed as maximum acceptable limit. Specimens completely covered by the patina well passed the check, while the less corroded and non-fully patinated specimens did not. This latter group includes specimens aged in Cl^- 1.5 mg L^{-1} , NO_3^- 1.5 mg L^{-1} , NO_3^- 10 mg L^{-1} , for all the ageing times, and in NO_3^- 25 mg L^{-1} for 276 cycles (see section 3.1). For these specimens, the analysis of the pickling solutions led to a significant overestimation of the total amount of metals in AR, with values more than 30% higher than the corresponding mass loss: their AR data were therefore not considered. For the specimens that passed the check, the amount of each metal retained in AR during the ageing in the different solutions is reported in Figure 5.

Taking into account that the total weight of metals in TRF always represents less than 3% of the mass loss and does not contribute to such overestimation, metals released in the weathering solutions can be reported and discussed for all the specimens (Figure 6, S5). As regards the amount of metals in TRF, it has to be considered that the experimental conditions here applied do not include mechanical stresses. If mechanical stresses were applied, part of the products that remain in patina would be probably lost as particulate fraction.

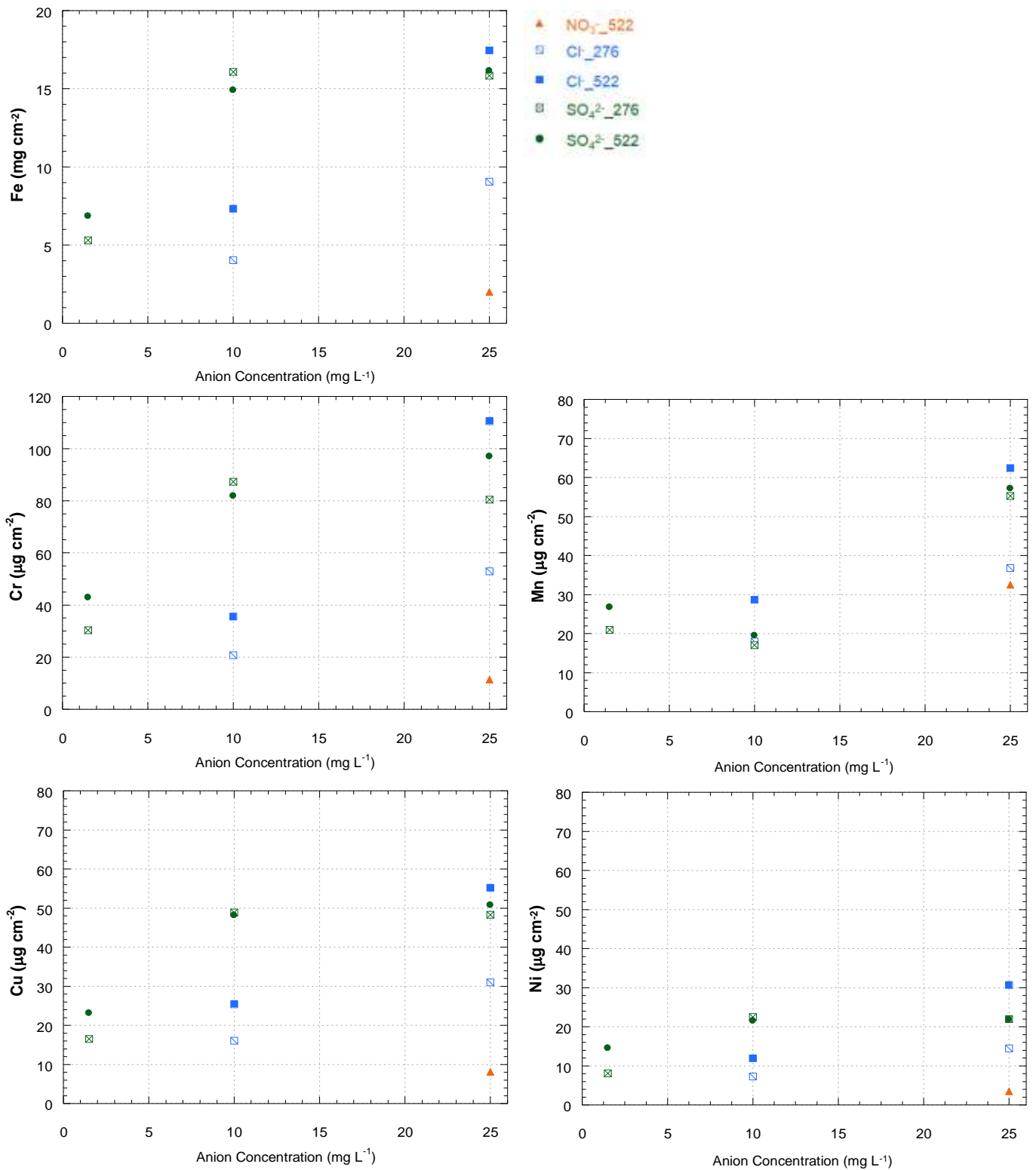


Figure 5. Fe (mg cm^{-2}), Cr, Mn, Cu and Ni ($\mu\text{g cm}^{-2}$) cumulatively retained in the Adherent Rust formed on WS specimens after 276 and 522 Cebelcor cycles in NO_3^- , Cl $^-$ and SO_4^{2-} solutions.

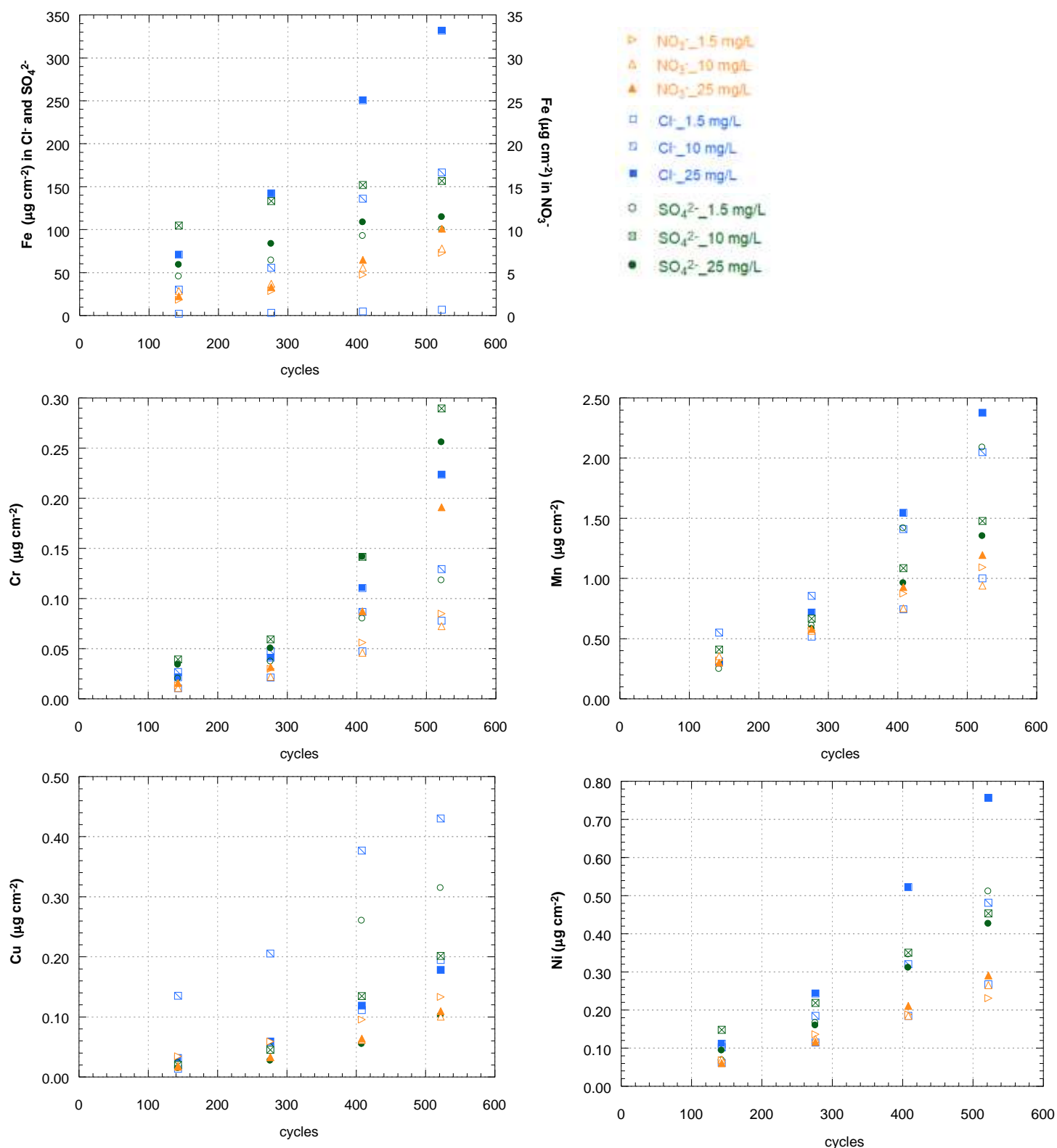


Figure 6. Fe, Cr, Mn, Cu and Ni ($\mu\text{g cm}^{-2}$) cumulatively released as TRF by WS specimens during the Cebelcor cycles in NO_3^- , Cl^- and SO_4^{2-} solutions.

As expected by the alloy composition, Fe is the most abundant metal in both patinas and solutions, with amounts 2 up to 3 order of magnitude higher than the other ones. It is therefore the Fe behaviour to define quantitatively the overall trends in both AR and TRF. Moreover, considering that the contribution of AR to

mass loss is always >97%, it is the Fe content in patinas to be mainly responsible for the corrosivity trends discussed in section 3.2 (crf. Figure 4 and 5 (Fe)).

The other alloying metals in AR follow trends, both over time and with anion concentrations, similar to those of Fe. In addition, their content tends to reflect the initial composition of the alloy, as shown by the relative percentages at the end of ageing (Figure 7a). Only adherent rust formed in the most concentrated NO_3^- solution (25 mg L^{-1}) seem to enrich in Mn (1.6% vs 0.38% in the bulk alloy).

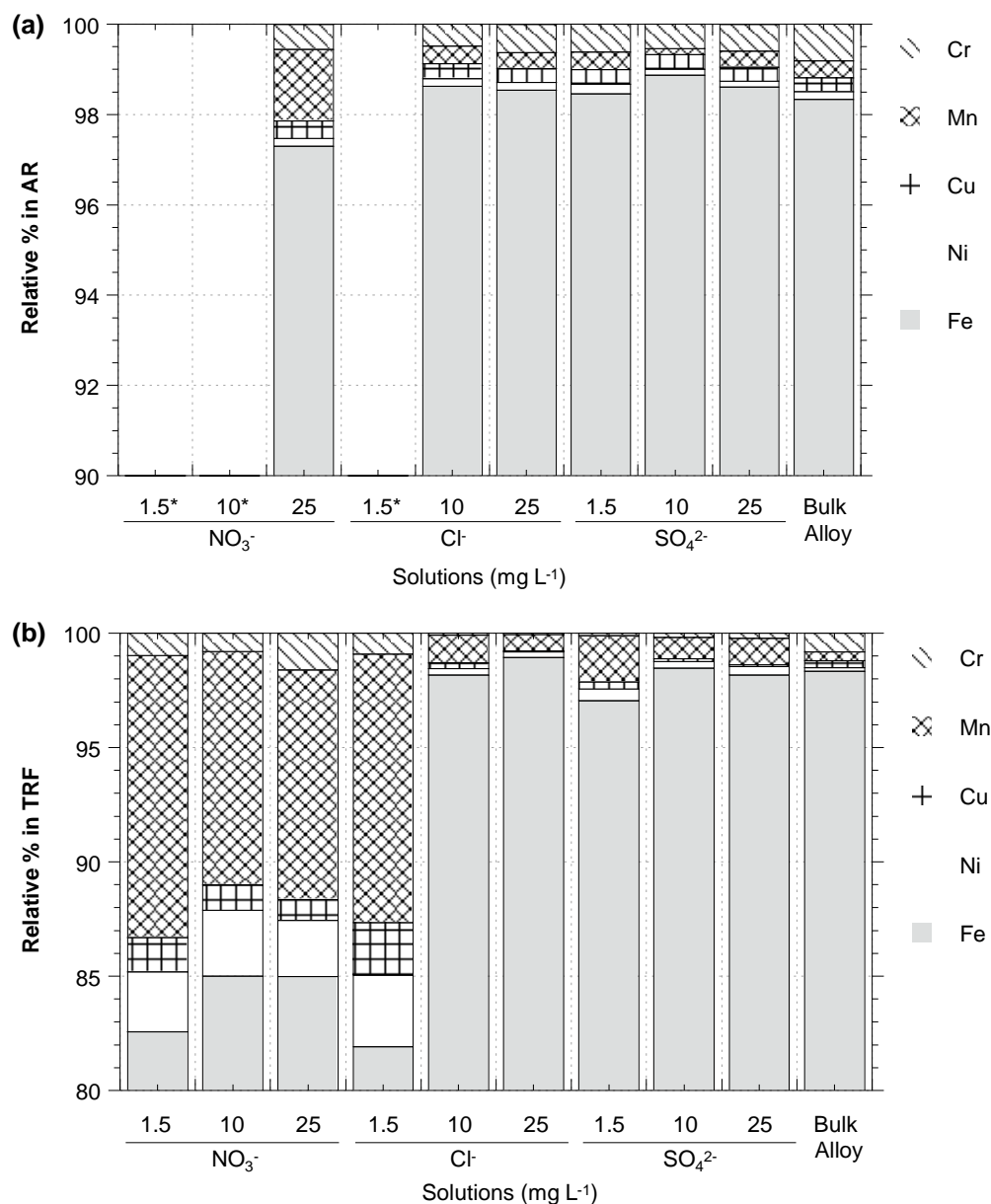


Figure 7. Relative percentage amount of Fe, Cr, Mn, Cu and Ni with respect to their sum in Adherent Rust (a) and in Total Released Fraction-cumulative amounts (b) for WS specimens aged in NO_3^- , Cl^- and SO_4^{2-} solutions for 522 Cebelcor cycles. The same relative percentage calculated for the bulk alloy is also reported in (a) and (b). Relative percentages marked with (*) were not calculated, according to the reasons explained in the text.

Considering metals in TRF, Fe release in NO_3^- solutions seems to be independent of their concentration during the first part of the ageing, and to exponentially increase with time ($R^2 > 0.997$) (Figure 6 (Fe)). Particularly, it seems to exist a threshold value of time and NO_3^- concentration (around 25 mg L^{-1}) beyond which not only mass loss (and likely Fe in patina), but also Fe release undergoes rapid acceleration. In any case, absolute Fe release in NO_3^- remain 1 up to 2 orders of magnitude lower than in Cl^- and SO_4^{2-} solutions.

In Cl^- solutions Fe release linearly increases with concentration and time ($R^2 > 0.98$), showing the same tendency of Fe in patina. Comparing the Fe trends over time, Cl^- seems to induce a decoupling between release, on one hand, and retention in patina and mass loss, on the other, slightly accelerating the first with respect to the seconds. Cl^- in the environment could therefore contribute more than the other anions to the general trend of runoff rates. In fact, while corrosion rates tend to globally decrease during the first years of exposure, runoff rates tend to remain quite constant over time, as observed during field exposure of several metals [32,33].

In SO_4^{2-} solutions, independently of the concentration, an immediate high release of Fe is recorded, which stabilizes over time according to a logarithmic trend ($R^2 > 0.98$). Increasing the concentration from 1.5 to 10 mg L^{-1} enhances Fe release, while a further increase up to 25 mg L^{-1} suppress it. Fe retained in patina follows the same tendencies.

What observed about the Fe behaviour in the different solutions can be explained taking into account that iron dissolves as Fe^{2+} , then Fe^{3+} is generated by aerial oxidation and participates to the formation of corrosion products. In aqueous solutions with pH in the range 5-8, as it is in this work, the Fe^{2+} oxidation rate is determined by the concentration of $\text{Fe}(\text{OH})_2$, increasing with pH. It was observed that the presence of anions lowers the oxidation rate in the order $\text{NO}_3^- > \text{Cl}^- > \text{SO}_4^{2-}$, due to the formation of Fe^{2+} complexes less prone to be oxidized with respect to the hydroxide [34,35]. Moreover, ones formed, Fe^{3+} can be complexed by the anions according to the following order of stability: $\text{SO}_4^{2-} \gg \text{Cl}^- > \text{NO}_3^-$ [14]. These combined effects, could explain the lower aggressiveness of NO_3^- solutions in regards to both the slower growth of the patinas and the lower release of iron. In fact, Cl^- and SO_4^{2-} reduce the oxidation rate of Fe^{2+} to Fe^{3+} less than NO_3^- . Moreover, via complexation, they can favour the formation of corrosion products [11,12], as well as the release of Fe^{3+} from iron oxides/hydroxides [36]. In the experimental conditions here applied, Fe in solution is always found mainly in the particulate fraction (from about 75-80% in Cl^- 1.5 mg L^{-1} and NO_3^- solutions, to more than 90% in SO_4^{2-} and in the remaining Cl^- solutions, on cumulative amounts) (Figure S5).

According to the discussed orders of influence, SO_4^{2-} promotes formation of Fe corrosion products (Figure 5) and Fe release more than Cl^- (Figures 6, S5), especially at the lowest concentrations (1.5 and 10 mg L^{-1}) and during the first phases of ageing. Over time, patinas developed in SO_4^{2-} solutions result relatively more protective and both processes tend to stabilize: after 522 cycles at the highest concentration (25 mg L^{-1}), Fe in patina became almost the same in SO_4^{2-} than in Cl^- , while Fe release one third less. The tendency of the patina to stabilize with increasing time and SO_4^{2-} concentration is in agreement with the detection of goethite (section 3.1) and with the findings of Tanaka et al. [11]. They actually demonstrated as the increase in the addition of SO_4^{2-} during the synthesis of steel rust from $\text{Fe}(\text{III})$ acidic solutions can inhibit the formation of rust particles.

Unlike Fe, the amounts of Cr, Mn, Cu or Ni released in NO_3^- , Cl^- and SO_4^{2-} solutions are of the same order of magnitude, even if generally lower in the NO_3^- ones (Figures 6). Their release tend to increase with time, following trends from linear to exponential. Exponential trends are particularly noticeable in the case of Cr. The effect of the anion concentration is more evident in Cl^- and SO_4^{2-} solutions, where an opposite tendency is generally observed. In fact, the increase in Cl^- concentration stimulates the release, while the increase in SO_4^{2-} concentration reduces or stabilizes it. This confirms again a beneficial effect of SO_4^{2-} in stabilising the patina also as regards the alloying metals release.

The relative percentages of metals released in the weathering solutions (Figure 7b) do not reflect the original composition of the alloy and highlight a clear preferential release of Mn and, secondly, of Ni. This occurs in all the solutions, but particularly in the group of the less aggressive ones (NO_3^- - all concentrations; Cl^- 1.5 mg L^{-1}), where Mn and Ni relative percentages increase respectively from 0.38 and 0.17% in the bulk alloy to 11 ± 1 and $2.8 \pm 0.3\%$ in TRF at the end of ageing. This significant preferential release of Mn is in agreement with the enrichment in Mn found in the adherent rust grown in NO_3^- 25 mg L^{-1} . This was the only case, within this group of solutions, for which it was possible to quantitatively analyse metals in AR. However, it is probable that also the other patinas of this group have an analogous enrichment. This hypothesis is supported by the relative percentages calculated on the basis of PF values. Due to its NAR content, PF is indeed the component of TRF that better reflect the composition of the patina and, in the less aggressive solutions, it shows a significant enrichment in Mn ($8 \pm 2\%$ vs 0.38% in the alloy) together with a less marked

enrichment in Ni ($2.4 \pm 0.4\%$ vs 0.17% in the alloy). Only in this group a slight preferential release of Cu is also detectable, especially in DF (Figure S5 (Cu)). These enrichments correspond to a relative decrease in Fe, while the Cr proportion remains analogous to that in the alloy.

In the remaining most aggressive solutions (Cl^- 1.5 and 10 mg L^{-1} ; SO_4^{2-} - all concentrations), the preferential release of Mn and Ni, although still evident, results less marked (relative percentages in TRF equal to $1.2 \pm 0.5\%$ and $0.3 \pm 0.1\%$ on average, respectively). This is probably due to the higher influence that the loss of NAR has on metal release in these solutions (crf. Figure S5(Fe)), where rust grows faster and thicker. In fact, in this group neither AR (Figure 7a) nor PF are significantly enriched in Mn and Ni, while DF continues to be. In these solutions, Mn and Ni enrichments occur with a corresponding relative decrease in Fe, Cu and especially Cr. Cr comes almost completely from fragments of NAR (Figure S5(Cr)) and its relative impoverishment both in PF and DF confirms its tendency to form insoluble products taking part in the stabilization of inner corrosion layers [4].

The general trend in preferential release is in agreement with the practical electrochemical series for metals in oxygenated aqueous environments. According to this series, Ni redox potential shifts below those of Cu, Cr and Fe, while Mn remains the less noble both in the thermodynamic and practical series [37]. Mn and Ni are also the metals for which the dissolved fraction is more significant (Figure S5). At the end of ageing it represents 30 to 65% of TRF for Mn and 20 to 55% for Ni. Cu shows more scattered values, with DF higher than 50% in the less aggressive solutions and from 7 to 40% in the other cases. Mn and Ni therefore not only show a preferential release, but also a preferential dissolution with respect to their content in the alloy. Their relative percentages in DF at the end of ageing reach on average $18 \pm 5\%$ and $3 \pm 1\%$, respectively. The lowest values are recorded in the SO_4^{2-} solutions, showing once more a positive effect of this anion on the formation of a more stable and protective patina.

A preferential dissolution of the same order of magnitude for both Mn and Ni with respect to Cr, Cu and Fe was found for weathering steel exposed in a urban coastal environment [38]. In that study, NO_3^- , Cl^- and SO_4^{2-} concentrations in atmospheric depositions ranged within 1.5 and 10 mg L^{-1} , being Cl^- the most concentrated and reaching occasionally peaks well higher than 25 mg L^{-1} . This confirms the ability of the applied accelerated test to reproduce atmospheric corrosion phenomena, allowing to distinguish among specific trends and contributions of each anion.

3.4 Multivariate data analysis

Experimental information in term of mass loss, metals cumulatively retained in patina and released in solution were elaborated through PCA (section 2.6). This allows the solutions to be grouped according to their main effects on weathering steel corrosion. Graphical results of PCA calculation are shown in the Loading Plot (Figure 8a) and in the Score Plot (Figure 8b), where the first two principal components, explaining 67% and 18% of the variance respectively, are plotted.

The first component (PC-1) is mainly related to the total extent of corrosion, positively connected especially to the growth of the patina (AR) and mass loss (ML). The variables connected to metal release (TRF) and retention in patina (AR) act instead on the second component (PC-2). All the released metals, except Cr, are positioned in the first quadrant. The released Cr, whose presence in TRF mainly derives from the detachment of NAR (section 3.3), is positioned in the fourth quadrant, close to the variables connected to the patina features (Figure 8a).

Comparing the Score Plot (Figure 8b) and the Loading Plot, it can be observed that solutions and related specimens appear divided into four groups, scattered through the graph according to the tendencies separately observed in the previous sections. Specifically, the solutions identified as less aggressive (i.e. NO_3^- - all concentrations; Cl^- 1.5 mg L^{-1}) form a quite compact group (orange-rimmed) positioned between the second and the third quadrant, and therefore scarcely influenced by all the aspects of the corrosion process.

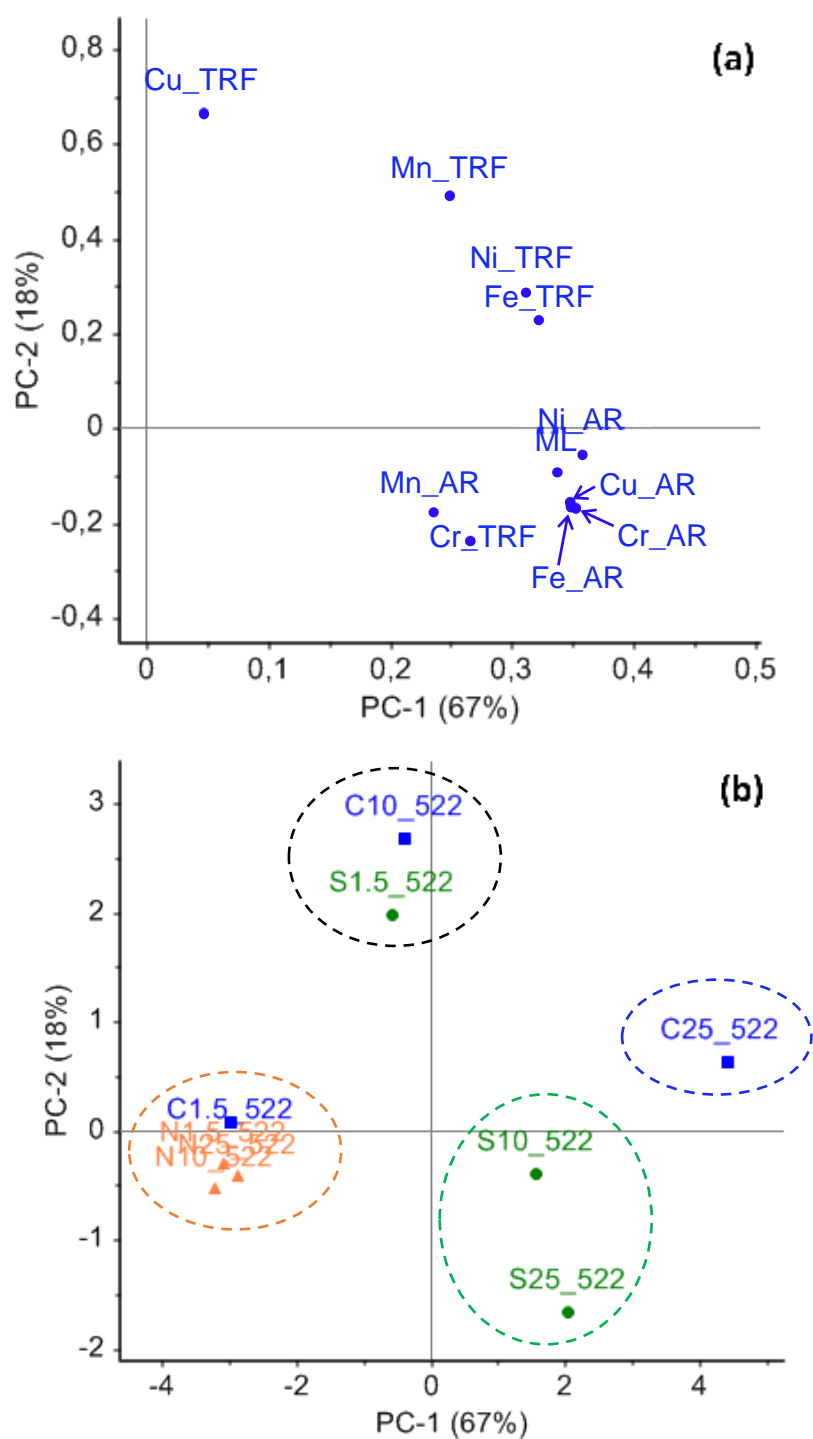
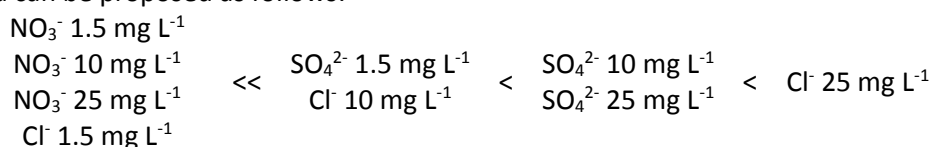


Figure 8. Loading (a) and Score (b) plot for the first (PC-1, explained variance 69%) and the second (PC-2, explained variance 16%) component of the PCA model. Variables included in the calculation are mass loss (ML), metals released in solutions (TRF) and metals retained in patinas (AR). Objects are labelled with a letter, referring to the weathering solution (N= NO_3^- , C= Cl^- , S= SO_4^{2-}) and a number (1.5, 10 or 25), referring to its concentration in mg L^{-1} ; the code 522 indicates the total number of Cebelcor ageing cycles.

A second group (black-rimmed), including $1.5 \text{ mg L}^{-1} \text{SO}_4^{2-}$ and $10 \text{ mg L}^{-1} \text{Cl}^-$, can be identified in the second quadrant, close to the first. This indicates that specimens aged in these solutions are relatively more influenced by the release of Fe and, in particular, of low-alloying elements. SO_4^{2-} solutions at 10 and 25 mg L^{-1}

¹ form a further group (green-rimmed) in the fourth quadrant, more connected to the retention of metals in the adherent rust and thus to the development of corrosion patinas. The last group (blue-rimmed) consists of a single object corresponding to the most concentrated Cl^- solution (25 mg L^{-1}). Its position is positively connected to both PC-1 and PC-2, and more shifted along PC-1 with respect to all the other groups. This suggests that, in this condition, corrosion can proceed at high extent and with a significant contribution of metal release, differently than in the corresponding SO_4^{2-} solution. This supports the hypothesis, previously made on the basis of Fe data, that Cl^- could contribute more than the other anions to metal runoff in the environment.

Summarizing, by considering all data and results from multivariate analysis, a corrosivity scale for the ageing solutions tested can be proposed as follows:



4. Conclusions

The role of the main atmospheric inorganic anions (NO_3^- , Cl^- and SO_4^{2-}) in weathering steel corrosion and metal release was investigated through an accelerated ageing test, performed at concentrations representative of mild to quite aggressive environments.

Results show that appearance, patina composition, corrosion rate and metal release are strongly influenced by the nature and concentration of the anions, which act on weathering steel with different kinetics and extent. Main conclusions can be summarised as follows:

- In all the weathering media, more than 97% of all the analysed metals remains in patina as adherent rust. The relative percentage of metals in the adherent rust reflect, in general, the initial composition of the alloy. Metals released in solution, on the contrary, follow different trend and show different proportion between dissolved and particulate fraction, depending on metal, weathering anion, anion concentration and time. In particular, Mn and Ni show a preferential release and dissolution, especially in NO_3^- and low concentrated Cl^- solutions.
- At the considered concentrations, the anions promote the growth and evolution of corrosion products in the following order: $\text{SO}_4^{2-} > \text{Cl}^- > \text{NO}_3^-$.
- NO_3^- is the least aggressive anion and only by overcoming a concentration and time threshold it start to slightly influence the corrosion process, leading to brown/dark patinas. Corrosion rate and total metal release result, respectively, one and one/two orders of magnitude lower than in the corresponding Cl^- and SO_4^{2-} solutions.
- Cl^- induces the development of poorly protective brown/orange patinas. Mass loss and total metal release tend to grow linearly with time and Cl^- concentration, giving no signs of stabilisation in the investigated ranges. The increase in Cl^- concentration tends to promote metal release more than metal retention in patina and mass loss. During outdoor exposure Cl^- could therefore contribute to metal runoff more than the other anions.
- In SO_4^{2-} solutions the corrosion processes show the highest kinetic and, even at the lowest concentration ($1.5 \text{ mg L}^{-1} \text{ SO}_4^{2-}$), reddish homogenous patinas develop rapidly. These patinas stabilize with time, as demonstrated by the slowdown of corrosion rate and metal release. Moreover, the increase in SO_4^{2-} concentration above 10 mg L^{-1} promotes goethite formation and tends to suppress both the growth of corrosion products and metal release. SO_4^{2-} ions appear therefore to favour the passivation of the alloy, even if a complete stabilization was not reached in the test period.
- Multivariate data analysis allowed to globally consider all the effects of the ageing conditions on weathering steel corrosion and to define the following corrosivity scale for the tested solutions: NO_3^- - all concentrations; $\text{Cl}^- 1.5 \text{ mg L}^{-1} << \text{Cl}^- 10 \text{ mg L}^{-1}$; $\text{SO}_4^{2-} 1.5 \text{ mg L}^{-1} < \text{SO}_4^{2-} 10 \text{ and } 25 \text{ mg L}^{-1} < \text{Cl}^- 25 \text{ mg L}^{-1}$.

Acknowledgments

The authors wish to gratefully acknowledge J.A. Jiménez and B. Chico from CENIM for XRD analyses and technical support, respectively.

References

- [1] W. Revie, H.H. Uhling, Corrosion and corrosion control: an introduction to corrosion science and engineering, 4th Ed., John Wiley & Sons, Inc., 2008. doi:10.1002/9780470277270.
- [2] EN 10025-5, Hot rolled products of structural steels - Part 5: Technical delivery conditions for structural steels with improved atmospheric corrosion resistance, (2005).
- [3] M. Morcillo, B. Chico, I. Díaz, H. Cano, D. de la Fuente, Atmospheric corrosion data of weathering steels. A review, Corros. Sci. 77 (2013) 6–24. doi:10.1016/j.corsci.2013.08.021.
- [4] M. Morcillo, I. Díaz, B. Chico, H. Cano, D. De Fuente, Weathering steels : From empirical development to scientific design. A review, Corros. Sci. 83 (2014) 6–31. doi:10.1016/j.corsci.2014.03.006.
- [5] K. Asami, M. Kikuchi, In-depth distribution of rusts on a plain carbon steel and weathering steels exposed to coastal–industrial atmosphere for 17 years, Corros. Sci. 45 (2003) 2671–2688. doi:10.1016/S0010-938X(03)00070-2.
- [6] S. Oesch, The effect of SO₂, NO₂, NO and O₃ on the corrosion of unalloyed carbon steel and weathering steel - the results of laboratory exposures, Corros. Sci. 38 (1996) 1357–1368.
- [7] A.U. Leuenberger-Minger, B. Buchmann, M. Faller, P. Richner, M. Zöbeli, Dose–response functions for weathering steel, copper and zinc obtained from a four-year exposure programme in Switzerland, Corros. Sci. 44 (2002) 675–687. doi:10.1016/S0010-938X(01)00097-X.
- [8] J. Aramendia, L. Gomez-Nubla, I. Arrizabalaga, N. Prieto-Taboada, K. Castro, J.M. Madariaga, Multianalytical approach to study the dissolution process of weathering steel: The role of urban pollution, Corros. Sci. 76 (2013) 154–162. doi:10.1016/j.corsci.2013.06.038.
- [9] J. Aramendia, L. Gomez-Nubla, K. Castro, J.M. Madariaga, Structural and chemical analyzer system for the analysis of deposited airborne particles and degradation compounds present on the surface of outdoor weathering steel objects, Microchem. J. 123 (2015) 267–275. doi:10.1016/j.microc.2015.07.004.
- [10] N.T. Lau, C.K. Chan, L.I. Chan, M. Fang, A microscopic study of the effects of particle size and composition of atmospheric aerosols on the corrosion of mild steel, Corros. Sci. 50 (2008) 2927–2933. doi:10.1016/j.corsci.2008.07.009.
- [11] H. Tanaka, N. Hatanaka, M. Muguruma, T. Ishikawa, T. Nakayama, Influence of anions on the formation of artificial steel rust particles prepared from acidic aqueous Fe(III) solution, Corros. Sci. 66 (2013) 136–141. doi:10.1016/j.corsci.2012.09.011.
- [12] H. Tanaka, N. Hatanaka, M. Muguruma, A. Nishitani, T. Ishikawa, T. Nakayama, Influence of anions on the structure and morphology of steel rust particles prepared by aerial oxidation of acidic Fe(II) solutions, Adv. Powder Technol. 27 (2016) 2291–2297. doi:10.1016/j.appt.2016.09.004.
- [13] T. Ishikawa, S. Miyamoto, K. Kandori, T. Nakayama, Influence of anions on the formation of β -FeOOH rusts, Corros. Sci. 47 (2005) 2510–2520. doi:10.1016/j.corsci.2004.10.016.
- [14] T. Kamimura, S. Nasu, T. Segi, T. Tazaki, H. Miyuki, S. Morimoto, T. Kudo, Influence of cations and anions on the formation of β -FeOOH, Corros. Sci. 47 (2005) 2531–2542. doi:10.1016/j.corsci.2004.10.014.
- [15] D.J. Jacob, D.A. Winner, Effect of climate change on air quality, Atmos. Environ. 43 (2009) 51–63. doi:10.1016/j.atmosenv.2008.09.051.
- [16] M. Pourbaix, J. van Muylder, A. Pourbaix, J. Kissel, An electrochemical wet and dry method for atmospheric corrosion, in: W.H. Ailor (Ed.), Atmos. Corros., John Wiley & Sons, New York, 1982: pp. 167–177.

- [17] P. Montoya, I. Diaz, N. Granizo, D. De La Fuente, M. Morcillo, An study on accelerated corrosion testing of weathering steel, *Mater. Chem. Phys.* 142 (2013) 220–228. doi:10.1016/j.matchemphys.2013.07.009.
- [18] N. Nutal, C.J. Gommès, S. Blacher, P. Pouteau, J.-P. Pirard, F. Boschini, K. Traina, R. Cloots, Image analysis of paerlite spheroidization based on the morphological characterization of cementite particles, *Imaga Anal Stereol.* 29 (2010) 91–98.
- [19] H. Sakihama, M. Ishiki, A. Tokuyama, Chemical characteristics of precipitation in Okinawa Island, Japan, *Atmos. Environ.* 42 (2008) 2320–2335.
- [20] L. Morselli, E. Bernardi, I. Vassura, F. Passarini, E. Tesini, Chemical composition of wet and dry atmospheric depositions in an urban environment: local, regional and long-range influences, *J. Atmos. Chem.* 59 (2008) 151–170.
- [21] A. Avila, M. Alarcon, Relationship between precipitation chemistry and meteorological situations at a rural site in NE Spain, *Atmos. Environ.* 33 (1999) 1663–1677.
- [22] L. Tositti, L. Pieri, E. Brattich, S. Parmeggiani, F. Ventura, Chemical characteristics of atmospheric bulk deposition in a semi-rural area of the Po Valley (Italy), *J. Atmos. Chem.* (2017). doi:10.1007/s10874-017-9365-9.
- [23] Y.S. Hedberg, S. Goidanich, G. Herting, I. Odnevall Wallinder, Surface-rain interactions: Differences in copper runoff for copper sheet of different inclination, orientation, and atmospheric exposure conditions., *Environ. Pollut.* 196C (2015) 363–370. doi:10.1016/j.envpol.2014.11.003.
- [24] I. Diaz, *Corrosion Atmosferica de Aceros Patinables de nueva generacion*, Universidad Complutense de Madrid, 2012. doi:10.1016/S0141-0229(03)00220-5.L.
- [25] ISO 8407, Corrosion of metals and alloys - Removal of corrosion products from corrosion test specimens, (2009).
- [26] J. Alcántara, B. Chico, J. Simancas, I. Díaz, D. de la Fuente, M. Morcillo, An attempt to classify the morphologies presented by different rust phases formed during the exposure of carbon steel to marine atmospheres, *Mater. Charact.* 118 (2016) 65–78.
- [27] R.M. Cornell, U. Schwertmann, *The Iron Oxides: Structure, Properties, Reactions, Occurences and Uses*, Wiley-VCH, 2003.
- [28] P. Refait, J.-M.R. Génin, The mechanisms of oxidation of ferrous hydroxylchloride β -Fe₂(OH)₃Cl in aqueous solution: The formation of akaganeite vs goethite, *Corros. Sci.* 39 (1997) 539–553. doi:10.1016/S0010-938X(97)86102-1.
- [29] C. Remazeilles, P. Refait, On the formation of β -FeOOH (akaganeite) in chloride-containing environments, *Corros. Sci.* 49 (2007) 844–857. doi:10.1016/j.corsci.2006.06.003.
- [30] M. Morcillo, J.M. González-Calbet, J.A. Jiménez, I. Díaz, J. Alcántara, B. Chico, A. Mazarío-Fernández, A. Gómez-Herrero, I. Llorente, D. de la Fuente, Environmental Conditions for Akaganeite Formation in Marine Atmosphere Mild Steel Corrosion Products and Its Characterization, *Corrosion.* 71 (2015) 872–886.
- [31] H. Xiao, W. Ye, X. Song, Y. Ma, Y. Li, Formation process of akaganeite in the simulated wet-dry cycles atmospheric environment, *J. Mater. Sci. Technol.* 34 (2018) 1387–1396. doi:10.1016/j.jmst.2017.06.020.
- [32] M. Faller, D. Reiss, Runoff behaviour of metallic materials used for roofs and facades - a 5-year field exposure study in Switzerland, *Mater. Corros.* 56 (2005) 244–249. doi:10.1002/maco.200403835.
- [33] Y.S. Hedberg, J.F. Hedberg, G. Herting, S. Goidanich, I.O. Wallinder, Critical Review: Copper Runoff from Outdoor Copper Surfaces at Atmospheric Conditions, *Environ. Sci. Technol.* 48 (2014) 1372–1381.
- [34] C. Sudakar, G.N. Subbanna, T.R.N. Kutty, Effect of anions on the phase stability of γ -FeOOH nanoparticles and the magnetic properties of gamma-ferric oxide derived from lepidocrocite, *J. Phys. Chem. Solids.* 64 (2003) 2337–2349. doi:10.1016/S0022-3697(03)00270-1.

- [35] B. Morgan, O. Lahav, The effect of pH on the kinetics of spontaneous Fe(II) oxidation by O₂ in aqueous solution – basic principles and a simple heuristic description, *Chemosphere*. 68 (2007) 2080–2084.
- [36] U. Schwertmann, Solubility and dissolution of iron-oxides, *Plant Soil*. 130 (1991) 1–25. doi:10.1007/BF00011851 Published: JAN 1991.
- [37] G. Bianchi, F. Mazza, Corrosione e protezione dei metalli, Associazione Italiana di Metallurgia, AIM, 2005.
- [38] S. Raffo, I. Vassura, C. Chiavari, C. Martini, M.C. Bignozzi, F. Passarini, E. Bernardi, Weathering steel as a potential source for metal contamination: metal dissolution during 3-year of field exposure in a urban coastal site, *Environ. Pollut.* 213 (2016) 571–584. doi:10.1016/j.envpol.2016.03.001.

Supplementary information

Influence of inorganic anions from atmospheric depositions on weathering steel corrosion and metal release

Elena Bernardi^{a,b*}, Ivano Vassura^{a,b}, Simona Raffo^a, Lara Nobili^a, Fabrizio Passarini^{a,b}, Daniel de la Fuente^c, Manuel Morcillo^c,

^a Department of Industrial Chemistry “Toso Montanari”, University of Bologna, Viale del Risorgimento 4, 40136 Bologna, Italy - elena.bernardi@unibo.it

^b Interdepartmental Center for Industrial Research (CIRI) Energy and Environment, University of Bologna, Via Angherà 22, 47900 Rimini, Italy

^c National Centre for Metallurgical Research (CENIM-CSIC), Avda. Gregorio del Amo, 8, 28040 Madrid, Spain

Supplementary information includes:

Figure S1. Microstructure of the weathering steel tested (1000x). Longitudinal section (a), transversal section (b). The following phases can be observed: ferrite (bright areas) and pearlite, the latter both in very fine grain size (light-brown areas) and in globular form (dotted areas). (p. S2)

Figure S2. Cebelcor test in the wet (a) and dry (b) positions. (p. S3)

Figure S3. Visual appearance of specimens aged in NO_3^- , Cl^- and SO_4^{2-} solutions at different concentrations for 276 and 522 Cebelcor cycles. (p. S4)

Figure S4. X-ray diffractogram of corrosion products formed on WS specimens aged in $25 \text{ mg L}^{-1} \text{NO}_3^-$, Cl^- and SO_4^{2-} solutions for 522 Cebelcor cycles (Counts x 1000). (p. S5)

Figure S5. Fe, Cr, Mn, Cu and Ni cumulatively released in the particulate (PF) and dissolved (DF) fractions ($\mu\text{g cm}^{-2}$) by WS specimens during the ageing (143, 276, 408, 522 Cebelcor cycles) in NO_3^- , Cl^- and SO_4^{2-} solutions. (p. S6)

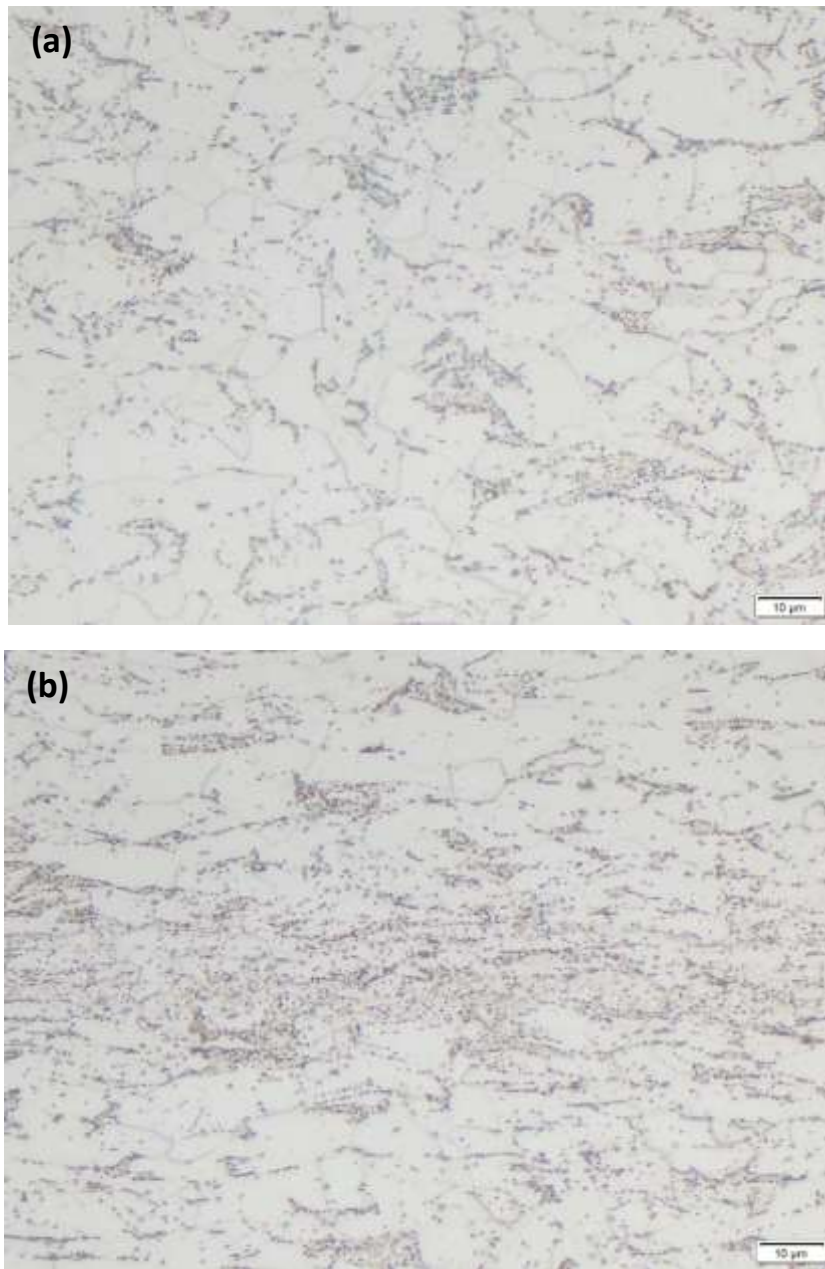


Figure S1. Microstructure of the weathering steel tested (1000x). Longitudinal section (a), transversal section (b). The following phases can be observed: ferrite (bright areas) and pearlite, the latter both in very fine grain size (light-brown areas) and in globular form (dotted areas).

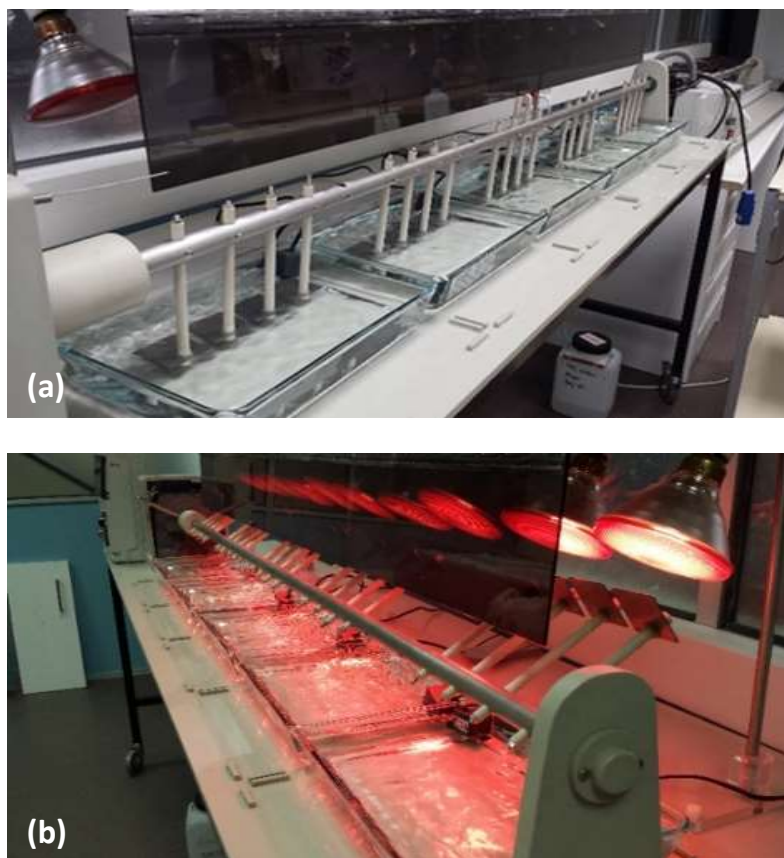


Figure S2. Cebelcor test in the wet (a) and dry (b) positions.



















		Anion Concentration		
	Ageing cycles	1.5 mg L ⁻¹	10 mg L ⁻¹	25 mg L ⁻¹
NO ₃ ⁻	276			
	522			
Cl ⁻	276			
	522			
SO ₄ ²⁻	276			
	522			

Figure S3. Visual appearance of specimens aged in NO₃⁻, Cl⁻ and SO₄²⁻ solutions at different concentrations for 276 and 522 Cebelcor cycles.

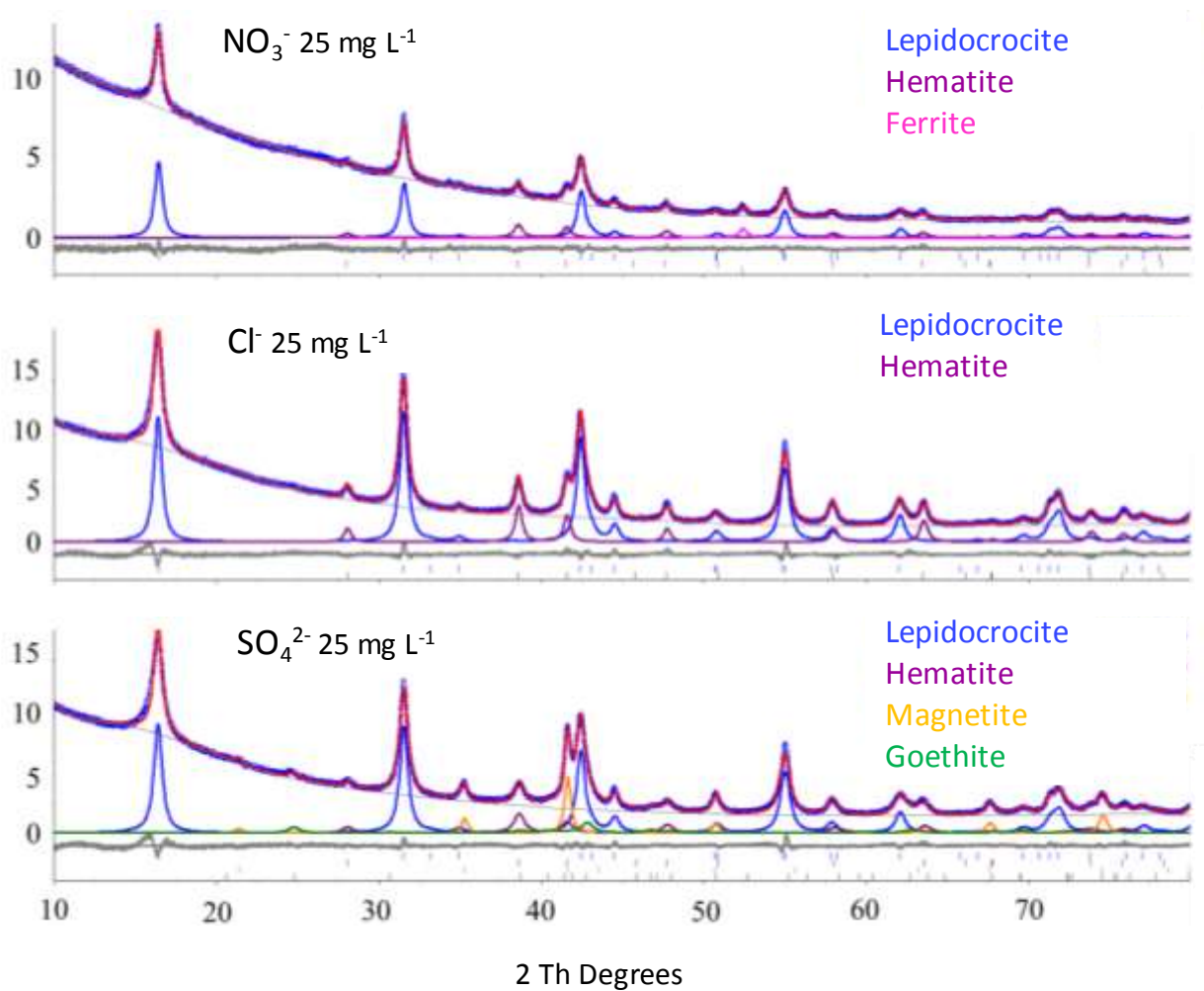


Figure S4. X-ray diffractogram of corrosion products formed on WS specimens aged in 25 mg L⁻¹ NO₃⁻, Cl⁻ and SO₄²⁻ solutions for 522 Cebelcor cycles (Counts x 1000).

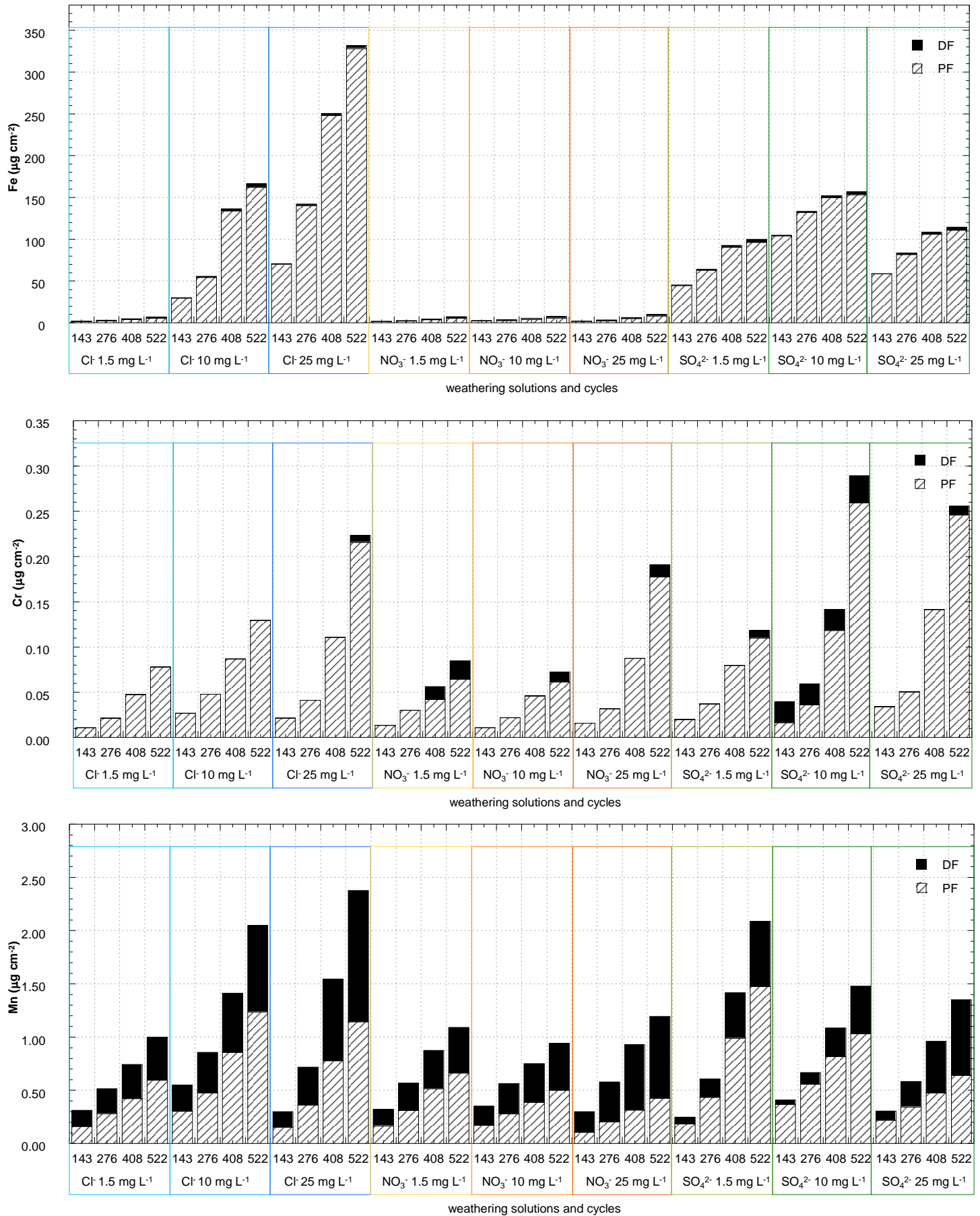


Figure S5 (follows in the next page)

Figure S5 (follows from the previous page)

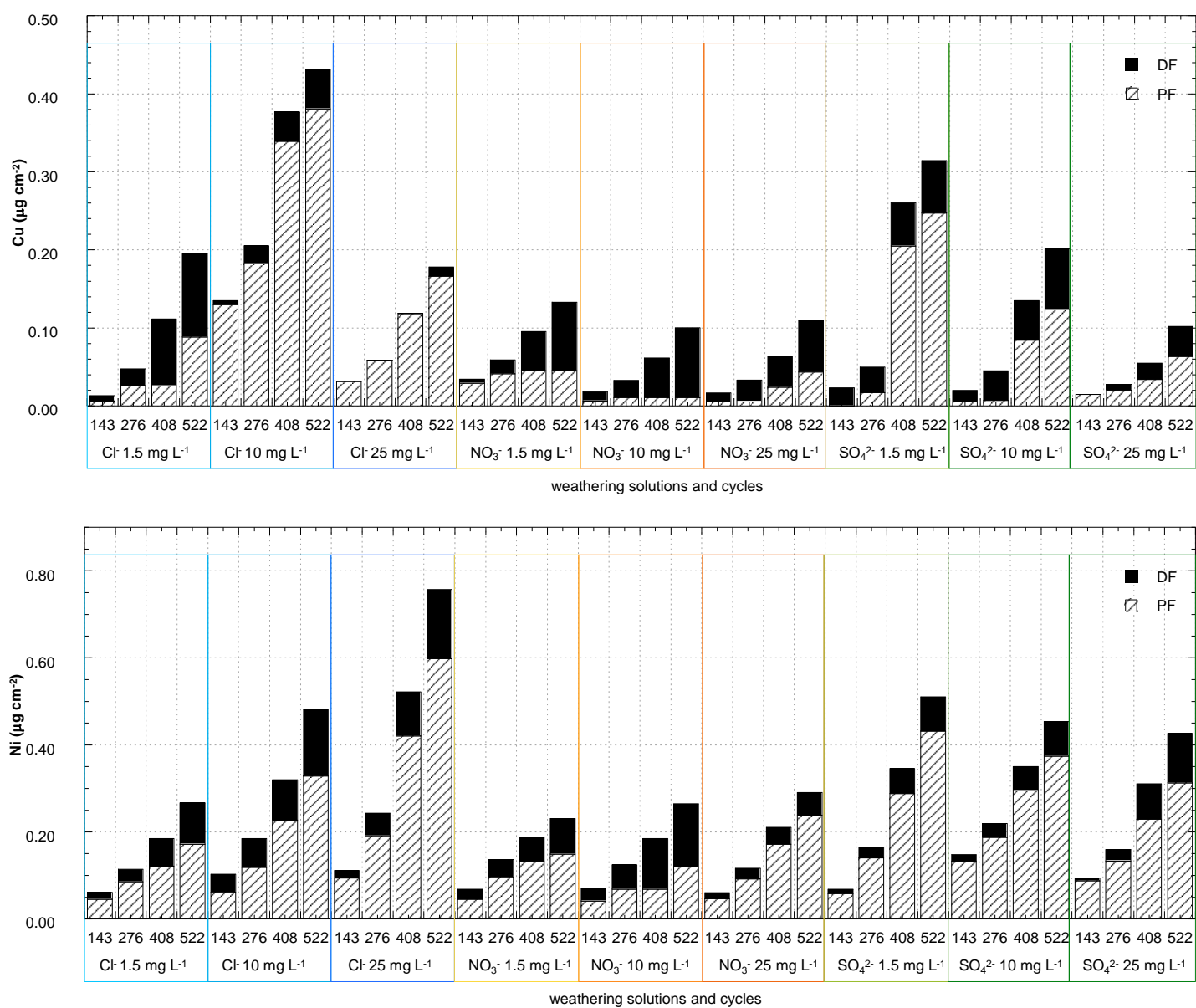


Figure S5. Fe, Cr, Mn, Cu and Ni cumulatively released in the particulate (PF) and dissolved (DF) fractions ($\mu\text{g cm}^{-2}$) by WS specimens during the ageing (143, 276, 408, 522 Cebelcor cycles) in NO_3^- , Cl^- and SO_4^{2-} solutions.